Mon. Not. R. astr. Soc. (1982) **200**, 1091–1111

Optical absorption lines in the high redshift BL Lac object 0215 + 015

J. C. Blades* *Anglo-Australian Observatory, PO Box 296, Epping, NSW 2121, Australia and Rutherford and Appleton Laboratories, Chilton, Didcot, Oxfordshire OX11 0QX*

R. W. Hunstead and H. S. Murdoch *School of Physics, University of Sydney, NSW 2006, Australia*

M. Pettini *Royal Greenwich Observatory, Herstmonceux Castle, Hailsham, East Sussex BN27 1RP*

Received 1982 January 8; in original form 1981 October 6

Summary. We present results from our study of 0215 + 015 (PKS 0215 + 015), the highest redshift and most luminous BL Lac object so far detected. Optical continuum measurements show that the object had brightened to 15.2 mag on 1980 September 10, thus confirming an overall variability range of more than 4 mag. Variations on a time-scale of $\leqslant 2$ months may also be present. A review of the published radio data indicates that 0215 + 015 has a core-halo or multi-component structure, similar to that found for the BL Lac 0735 + 178.

Four absorption redshift systems occur with $z_a = 1.254$, 1.345, 1.549 and 1.649. The $z_a = 1.345$ system exhibits a rich, mixed-ionization spectrum whilst the other three are predominantly C IV systems. All four show complex structure when observed at high resolution (~ 0.65 Å FWHM). Most remarkable are the $z_a = 1.549$ system which splits into three C IV components with average separation, $\overline{\Delta v} \sim 130\,\mathrm{km\,s^{-1}}$ and the $z_a = 1.649$ system to which we fit seven C IV components with $\overline{\Delta v} \sim 110\,\mathrm{km\,s^{-1}}$. Individual C IV clouds are narrow, having internal velocity dispersions (b values) in the range $15–55\,\mathrm{km\,s^{-1}}$, the lower values being similar to that produced by thermal broadening in gas at 10^5 K. Column densities are in the range $N(\mathrm{C\,IV}) = 2–20 \times 10^{13}\,\mathrm{cm^{-2}}$.

Possible origins of the absorption systems are discussed. Column densities of the $z_a = 1.345$ system are very similar to those found for our Galaxy in sight-lines towards the Magellanic Clouds, and an origin in an intervening galaxy seems almost certain for this system. The velocity structure and line-widths of the 1.649 system are less plausibly due to intervening galaxies, but are consistent with the intrinsic absorption model of Dyson, Falle & Perry (1980).

* Now at ESA Satellite Tracking Station, Villafranca del Castillo, PO Box 54065, Madrid, Spain.

1 Introduction

The radio source 0215+015 (PKS 0215+015) was identified from the Palomar Sky Survey (PSS) by Bolton & Wall (1969, 1970) as an 18.5 mag QSO and a finding chart is given in both papers. The optical position (1950.0) measured by us from the PSS O print is:

RA = $02^h\ 15^m\ 14^s.15 \pm 0^s.03$, Dec = $+01°\ 30'\ 59''.9 \pm 0''.4$.

The first recorded optical spectra of 0215 + 015 were reported by Wills & Lynds (1978) using the Kitt Peak 2.1-m reflector and image-tube spectrograph. Their measurements were made between 1970 April and 1972 October at a spectroscopic resolution of ~ 10 Å. They reported that 'three well-exposed spectrograms fail to reveal any consistent evidence for emission lines'. There was no mention of absorption lines.

The object is optically variable. It was not visible at a limiting magnitude ~ 19.5 on the two-colour plate of the relevant field taken in 1968 by Bolton & Wall (1969). A decade later Gaskell (1978, 1982) reported that the object had brightened to around 16 mag. As discussed later, 0215+015 appears also to show radio variability.

Gaskell's optical work on 0215+015 at Lick Observatory resulted in the discovery of rapidly variable polarization of up to 37 per cent and confirmed the absence of emission lines. These characteristics, and the variability, clearly indicate that 0215+015 should be classified as a BL Lac object.

1.1 RADIO DATA

The radio spectrum of 0215+015 is shown in Fig. 1. The points at 1400, 2700 and 5009 MHz are from Wall (1972) and the point at 8.083 GHz is from Wills (1979). The 318 and 606 MHz points are from Condon & Jauncey (1974) and have been adjusted upward slightly to a flux density scale consistent with the Wyllie scale at 408 MHz (Wyllie 1969). The 408 MHz point is from the *Molonglo Reference Catalogue* (Large *et al.* 1981). Other measurements at frequencies up to 2.7 GHz are consistent with Fig. 1 (see Gaskell 1982, for references).

The points joined by the broken line in Fig. 1 represent results obtained with the Jodrell Bank interferometer by Bentley *et al.* (1976) at 962 and 1666 MHz. The latter result is from

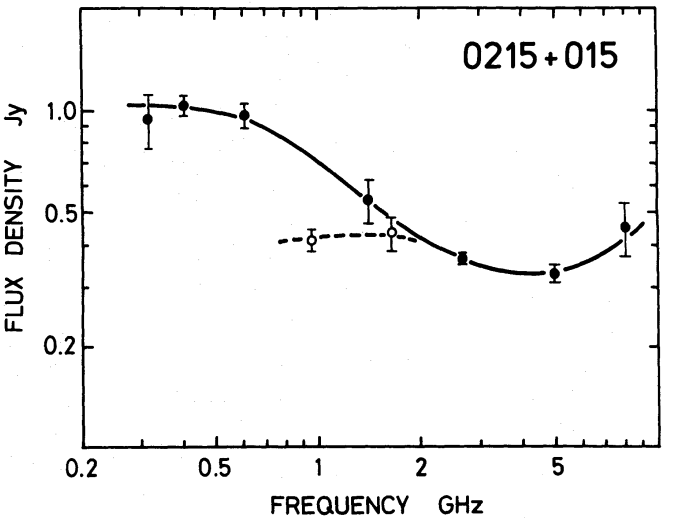

Figure 1. The radio spectrum of 0215+015. Solid points represent pencil-beam measurements made at Arecibo, Molonglo and Parkes (see text). Open circles joined by a dotted line represent Jodrell Bank interferometer results (Bentley *et al.* 1976).

a source component < 0.1 arcsec which evidently accounts for most of the flux density at that frequency. The lower frequency results suggest a more extended but still fairly compact component. Briggs & Wolfe are also reported by Gaskell (1982) as finding a compact component of 0.22 ± 0.04 Jy at 1400 MHz from VLBI observations with 0.02 arcsec fringe spacing. This represents about half of the flux density at this frequency in the component detected at Jodrell Bank. It thus seems likely that 0215+015 has a core-halo or multi-component structure as found by Cotton *et al.* (1980) for 0735+178, despite in that case, an apparently flat spectrum over a wide range of frequency.

None of the above results gives any firm indication of radio variability. However, a VLA measurement at 4.885 GHz by J. J. Condon (private communication) in 1980 December indicates an unresolved source (< 0.1 arcsec) of 0.70 ± 0.02 Jy. It would seem therefore that 0215+015 has brightened significantly at high frequency.

1.2 ABSORPTION SPECTRUM

Gaskell (1978) reported the discovery of a number of strong absorption lines in the optical spectrum of 0215+015 which indicated a well-defined low-ionization absorption line system at a redshift of 1.345, as well as two unidentified broad absorption features. At higher resolution (4 Å) Gaskell (1982) has since shown that these features are C IV doublets at absorption redshifts of 1.549 and 1.649. These are the highest redshift absorption systems reported for a BL Lac object. The only other case of a high-ionization absorption system in a BL Lac object is 1309−216 (Blades, Murdoch & Hunstead 1980) which has three C IV absorption systems at redshifts 1.361, 1.489 and 1.491. In the strongest of these $z_a = 1.489$, Si II and Si IV are also detected.

1.3 NEW SPECTROSCOPIC DATA

The current brightness of 0215+015 makes it an ideal object for detailed study of the relative abundances and ionization of the absorption line systems. Accordingly, we have embarked since 1979 October on an extensive observing programme utilizing the high-resolution capabilities of the 3.9-m Anglo-Australian telescope (AAT). In this paper we present the results of our observations to date obtained at medium and high resolution with the Image Photon Counting System (IPCS) (Boksenberg 1978) and at low resolution using the Image Dissector Scanner (IDS) (Robinson & Wampler 1972). We have discovered complex structure in both high-redshift C IV systems and also resolved structure in those lines of the $z_a = 1.345$ system which have been observed at sufficiently high resolution (~ 0.65 Å). A fourth C IV system has been found at redshift $z_a = 1.254$. First results of our analysis of the absorption line strengths and profiles are presented.

2 Spectroscopic observations and reduction

2.1 MEDIUM AND HIGH RESOLUTION DATA (IPCS)

The high-resolution optical spectroscopy presented in this paper was carried out at the $f/8$ Cassegrain focus of the AAT using the RGO spectrograph and IPCS. The observations were made with various combinations of gratings and cameras (25 and 82 cm focal lengths) during several observing sessions over one year starting in 1979 October. The journal of observations is given in Table 1.

In the observations of 1979 October and 1980 October the object was regularly beam-switched between two IPCS photocathode positions with the same total integration time in

Table 1. 0215+015: Journal of observations.

Date (UT)	Spectrograph + Detector	Camera (cm)	Grating (grooves/mm)	Spectral Region (Å)	Int (min)	Seeing (arcsec)	Actual slit width (arcsec)	FWHM: (Å)
1979 Oct 27.5	RGO + IPCS	25	1200B†	3400–4400	60	2	1.4	1.5 (M2
1979 Nov 1.6	RGO + IPCS	82	1200B	3910–4210	83	⩽1	0.7	0.66 (H
1979 Dec 25.4★	RGO + IPCS	25	600V	5000–7400	17	~1	0.8	3 (M1)
1980 Sep 10.7	B & C + IDS	–	600	3100–6600	16	3.5	2.0	11
1980 Oct 9.6	RGO + IPCS	25	1200R (II)	3450–3820	261	2.5	1.4	0.64 (H
1980 Nov 6.6	B & C + IDS	–	600	3100–6600	40	2.9	1.8	11

★ This spectrum was obtained for us by D. C. Carter (AAO).
† The grating notation used with the RGO spectrograph is described by Blades (1980).
‡ The shorthand notation given in brackets is used for subsequent reference to each spectrum.

each position. The other observations were made with the object held at one position in the slit, a composite sky spectrum being obtained from adjacent IPCS pixels. Typically, individual integrations were between 500–1000 s. For wavelength calibration frequent comparison spectra were taken using a Cu–Ar hollow cathode lamp. The red spectrum of 0215+015 was taken at our request by Dr D. Carter (AAO). It is a short integration (100 s) but nevertheless provides a useful check on the presence of absorption lines over this spectral region.

2.2 LOW RESOLUTION DATA (IDS)

In addition to these data, two low-resolution spectra (FWHM = 11 Å) of 0215+015 were obtained at the $f/15$ Cassegrain focus with the Boller & Chivens spectrograph and IDS (blue-sensitive image tube). The first of these scans (1980 September 10) was a short integration intended only to check the brightness of 0215+015 prior to the October 9 IPCS observation. The second scan (1980 November 6) was a longer integration made with the spectrograph slit oriented in the direction of the atmospheric dispersion in order to confirm a tentative identification of Lyα absorption near 3200 Å in the highest redshift system. On each occasion the same standard stars (L930−80, L745−46A) from Oke (1974) were observed for flux density calibration. Both the IPCS and IDS data were reduced using the Scanner Data Reduction System (SDRSYS) largely developed at the AAO by Straede (1980).

3 Results

3.1 CONTINUUM MEASUREMENTS

We have used the IDS scans to estimate magnitudes and spectral indices using the techniques described by Hunstead & Murdoch (1980). Briefly, this involves making a first-order correction to the raw spectra for the light lost from the spectrograph apertures due to the combined effects of seeing and atmospheric dispersion. A straightforward numerical integration is carried out for both the object and standard star data, based on the aperture size and orientation, the zenith and parallactic angles, the assumed guiding wavelength and the measured seeing FWHM; the seeing profile is assumed to be Gaussian.

Table 2. 0215+015: Continuum measurements from the IDS scans.

UT date	m_{5500} (corrected)	$\alpha_{4000-6000}$ (corrected)	Standard star
1980 Sept 10.7	15.2	1.7	L930 – 80
	15.3	2.1	L745 – 46A
1980 Nov 6.6	16.1	1.8	L930 – 80
	16.2	1.5	L745 – 46A

The continuum magnitude at 5500 Å (m_{5500}) and the continuum spectral index α (defined in the sense $f_\nu \propto \nu^{-\alpha}$) between 4000 and 6000 Å have been determined using each standard star separately and the results are given in Table 2. Although the corrections to m_{5500} ranged from +0.5 to −0.7 mag, the consistency between the corrected magnitudes for each epoch is very good and is taken as vindication of the procedures adopted. The difference of 0.9 ± 0.3 mag (estimated rms error) between the two observations suggests a significant change in brightness on a time-scale of $\leqslant 2$ months. Furthermore, the 1980 September 10 magnitude of 15.2 confirms an overall variability range of more than 4 mag for 0215+015.

The difference in spectral index between the two epochs is not significant and the scatter simply reflects the uncertainties in the calibration procedure. The separate estimates in Table 2 are consistent with a mean index of 1.8 ± 0.3 which agrees with Gaskell's (1982) values of 2.11 and 1.76. Neither of the IDS scans shows evidence for emission features.

An uncorrected $\log f_\nu$: $\log \lambda$ plot of the 1980 November 6 scan of 0215+015 is shown in Fig. 2. This plot covers the range 3100–6600 Å. The power-law continuum appears to be well-maintained over this range although extension of the flux density calibration below 3300 Å relies on extrapolation of Oke's (1974) data for L745 – 46A.

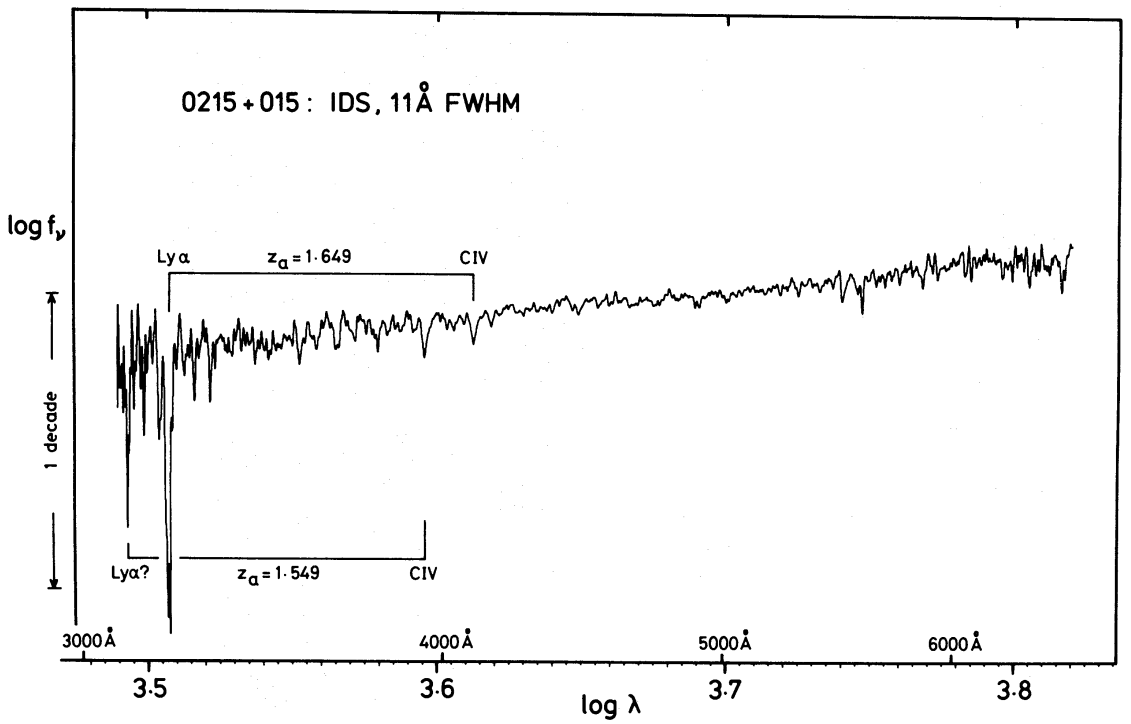

Figure 2. Low-resolution (11 A) IDS scan of 0215+015 (1980 November 6). Log f_ν is plotted against log λ prior to applying corrections for light loss as discussed in the text. Only the *scale* of the ordinate is therefore indicated.

3.2 ABSORPTION LINES

We identify four definite absorption systems based on the lines listed in Table 3, where heliocentric vacuum wavelengths are given for all lines detected in the low-resolution IDS and medium-resolution IPCS spectra (M2 = 1.5 Å FWHM, M1 = 3 Å FWHM). One system at $z_a = 1.34450 \pm 0.00004$ is a rich mixed-ionization system, including lines from widely different ionization stages of the same element (e.g. C I and C IV). In the other systems, at $z_a = 1.2542 \pm 0.0001$, $z_a = 1.5489 \pm 0.0001$ and $z_a = 1.649 \pm 0.002$, the C IV doublet lines are the most prominent features (apart from Lyman α); we refer to these as high-ionization systems. The redshift values have been determined from the rest wavelengths given by Morton (1978), adjusted above 2000 Å to vacuum values, and from heliocentric-corrected, observed wavelengths also adjusted to vacuum values. The observed wavelengths are from

Table 3. 0215+015: Absorption line list.

λ_{obs}^{helio} (vac) (Å)	Ident	λ_{rest} (vac) (Å)	z	W_λ (obs)* (Å)	
$z = 1.254$ system					
3490.09	C IV	1548.19	1.25431	1.2 (M2);	0.97 (H1)
3495.69	C IV	1550.76	1.25418	0.9 (M2);	0.75 (H1)
$z = 1.345$ system					
3579.45	Si II	1526.71	1.34455	2.02 (M2);	1.92 (H1)
3630.01	C IV	1548.19	1.34468	0.63 (M2);	0.69 (H1)
3635.70	C IV	1550.76	1.34446	0.71 (M2);	0.53 (H1)
3771.21	Fe II	1608.46	1.34461	0.59 (M2);	0.75 (H1)
3885.30:	C I	1656.93	1.34488:	0.54 (M2)	
3917.38	Al II	1670.79	1.34463	1.83 (M2);	1.64 (H2)
4238.10:	Si II	1808.01	1.34407:	0.34 (M2)	
4349.25:	Al III	1854.72	1.34496:	0.32 (M2)	
4368.95:	Al III	1862.79	1.34538:	0.30 (M2)	
5496.31	Fe II	2344.21	1.34463	2.1 (M1)	
5566.52	Fe II	2374.46	1.34433	0.9 (M1)	
5586.02	Fe II	2382.76	1.34435	4.5 (M1)	
6064.61	Fe II	2586.65	1.34458	2.4 (M1)	
6096.23	Fe II	2600.18	1.34454	3.4 (M1)	
6555.82	Mg II	2796.35	1.34442	4.4 (M1)	
6572.20	Mg II	2803.53	1.34426	4.0 (M1)	
$z = 1.549$ system					
3116 : :	Ly α	1215.67	1.56:	5 (IDS)	
3946.21	C IV	1548.19	1.54892	2.48 (M2);	2.53 (H2)
3952.59	C IV	1550.76	1.54881	1.83 (M2);	1.96 (H2)
$z = 1.649$ system					
3218 :	Ly α	1215.67	1.647:	15 (IDS)	
3533.17	C II	1334.53	1.64750	0.85 (M2);	1.04 (H1)
3690.19	Si IV	1393.76	1.64765	0.63 (M2);	0.60 (H1)
3717.1:	Si IV	1402.77	1.6499:	0.40 (M2)	
4100.5	C IV	1548.19	1.6486		2.02 (H2)
4106.1	C IV	1550.76 1548.19	–		1.97 (H2)
4111.4	C IV	1550.76	1.6512		0.32 (H2)

* Sources of the equivalent widths are IDS where noted (at a resolution of 11 Å) or IPCS according to the following code:

M1 = 3 Å, M2 = 1.5 Å, H1 = 0.64 Å and H2 = 0.66 Å.

M1 and M2 except for the $z_a = 1.254$ system where they are from H1. The detection limit for a narrow absorption line is $W_\lambda \simeq 0.3$ Å for the blue region (M2) and $W_\lambda \simeq 0.7$ Å in the 5000–7000 Å region (M1). There is an unidentified line with $W_\lambda \simeq 0.5$ Å at 3854.8 Å. Gaskell (1982) reports three unidentified lines at 3493.9, 3930 and 6527.9 Å. The first of these corresponds with the C IV doublet at $z_a = 1.254$. The second line may correspond with a probable Ca II *K* line detected at 3933.4 Å in our high-resolution spectrum (H2), although the equivalent width of 0.3 Å is just below Gaskell's detection limit. We do not confirm the third line at 6527.9 Å.

Table 3 also contains equivalent widths from both the medium- and high-resolution data. The medium-resolution spectrum covering the range 3400–4400 Å is illustrated in Fig. 3. This spectrum has been normalized to remove the instrumental response, thereby providing a flat continuum for the absorption lines.

At 1.5 Å resolution, lines belonging to the three lower redshift systems are all single whereas the highest redshift C IV is obviously broad and complex. However, when the same lines are studied at high resolution this simple picture changes. Double structure is found in the higher resolution scans of lines belonging to the $z_a = 1.345$ system. This is shown in Fig. 4 which illustrates the higher resolution IPCS spectrum in the wavelength range 3500–3800 Å and in Fig. 5 where strong lines in the $z_a = 1.345$ system are shown on an expanded scale. Triple structure at a velocity separation of 130 km s^{-1} occurs for the $z_a = 1.549$ C IV system (see Fig. 6). Finally, the $z_a = 1.649$ C IV system which is shown in Fig. 7 remains exceedingly complex and is not properly resolved even at 0.66 Å resolution; as discussed later, we ascribe seven C IV components to this feature.

Absorption line systems in the spectra of QSOs and BL Lacs are often found to show complex structure when observed at sufficiently high resolution and 0215+015 is a further example of this. Other well-studied cases include the BL Lac object 0735+178 (Boksenberg, Carswell & Sargent 1979) which exhibits multiple structure in the Mg II λλ2796.35,

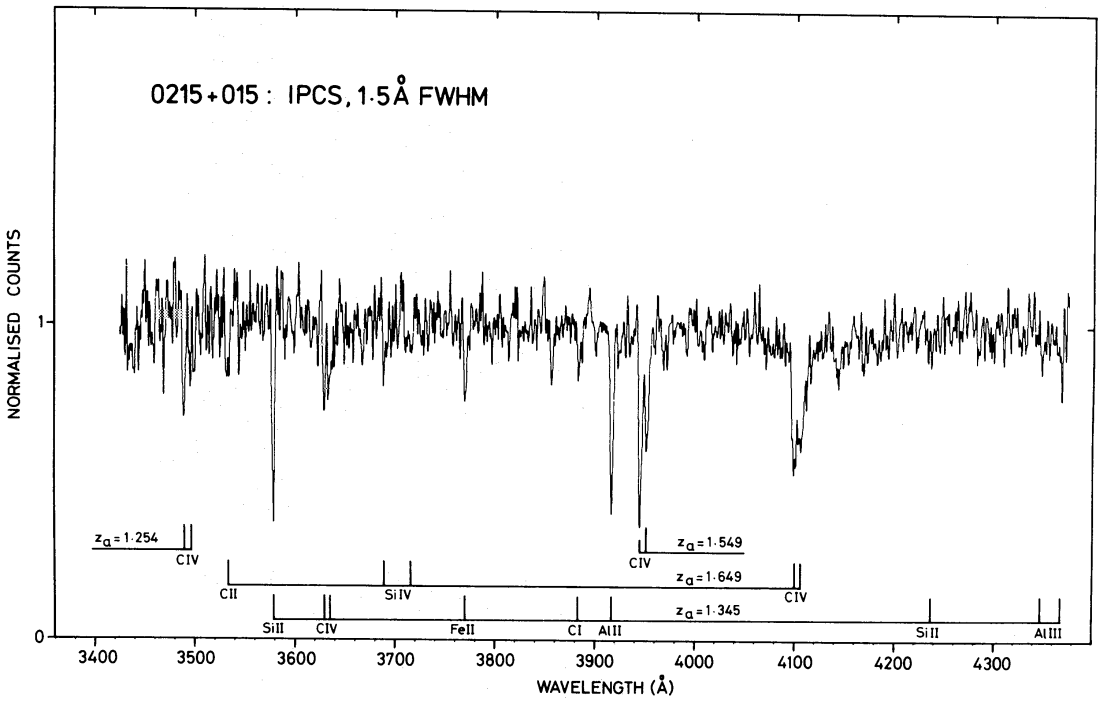

Figure 3. Medium-resolution (1.5 Å FWHM) IPCS spectrum of 0215+015 obtained on 1979 October 27. The spectrum has been normalized by dividing the raw spectrum by a smooth approximation to the continuum level.

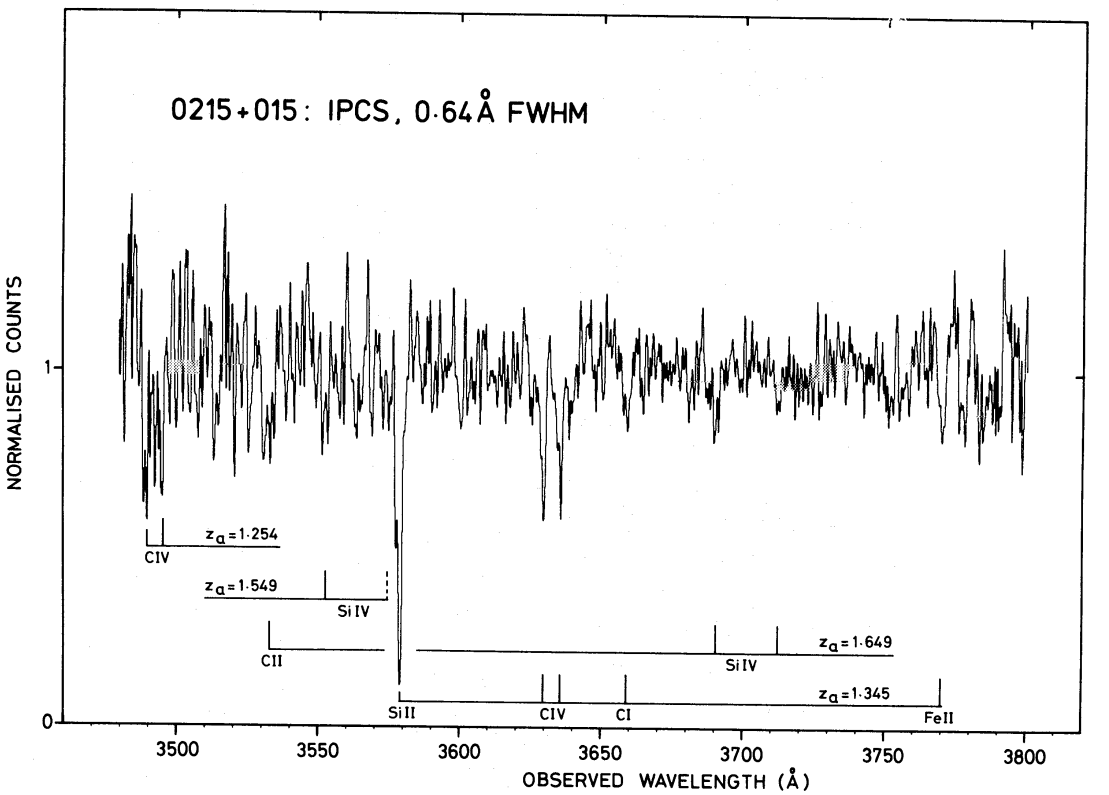

Figure 4. High-resolution (0.64 Å FWHM) IPCS spectrum of 0215+015 obtained on 1980 October 9. The continuum has been normalized in the same way as Fig. 3.

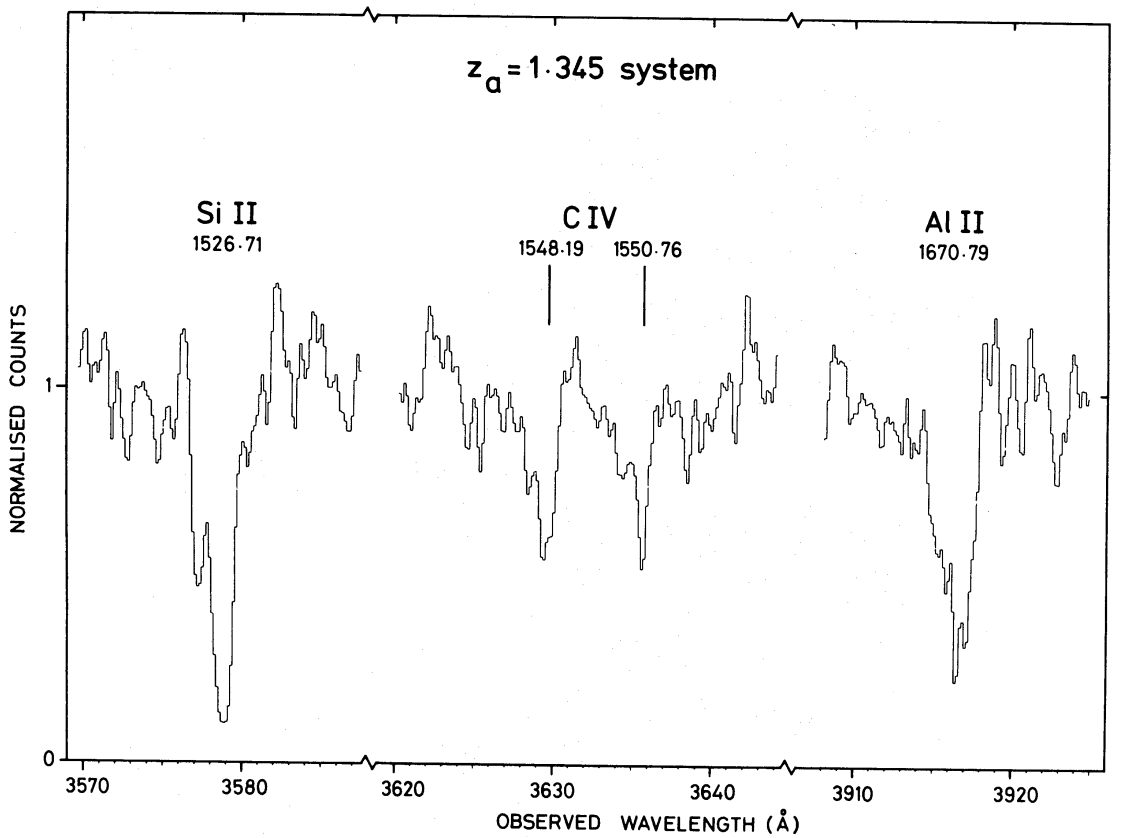

Figure 5. A montage of the strongest UV lines in the $z_a = 1.345$ system at high resolution. The Si II and C IV lines are expanded portions of Fig. 4 and the Al II line is from the 1979 November 1 spectrum (0.66 Å FWHM). Note that the abscissa is the observed wavelength in the air.

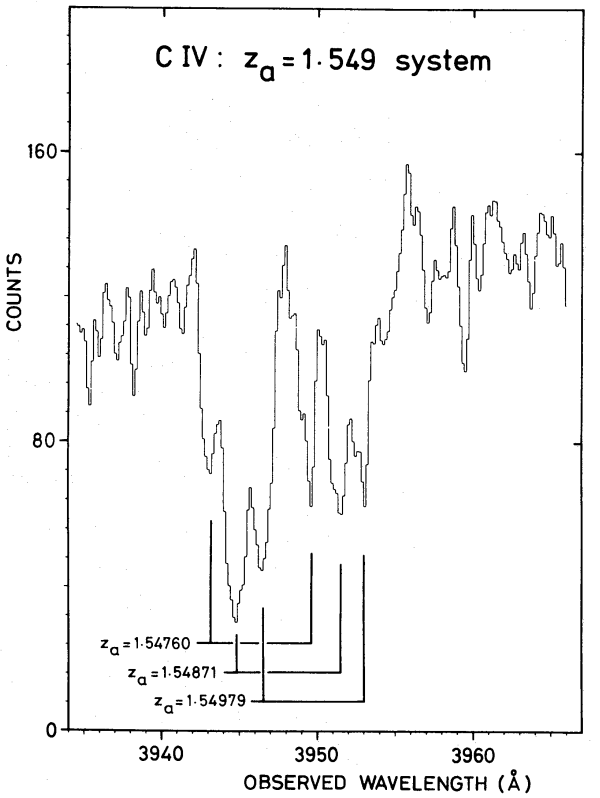

Figure 6. Splitting of the C IV doublet in the z_a = 1.549 system into three sub-systems at a resolution of 0.66 Å FWHM (1979 November 1 observation). Raw counts are plotted as a function of air wavelengths.

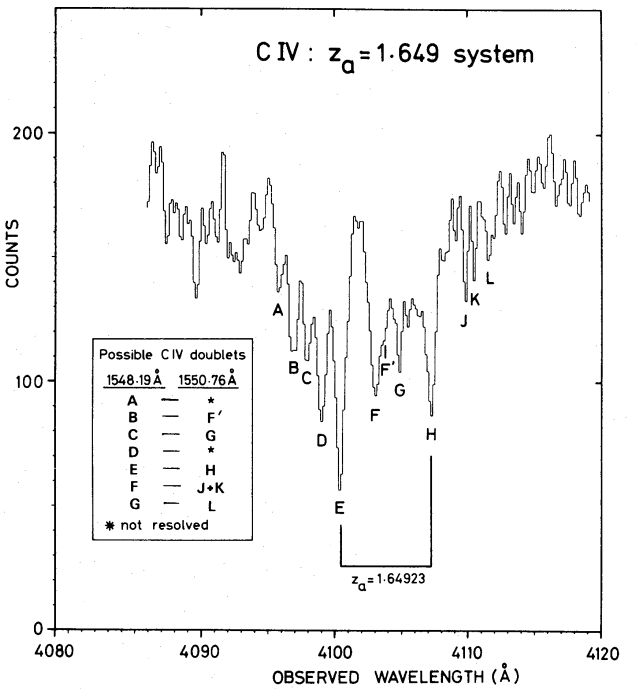

Figure 7. Complex structure of C IV in the z_a = 1.649 system from the same observation as in Fig. 6. The inset box lists pairs of features which we suggest as possible C IV doublets.

2803.53 doublet at $z_a = 0.424$ and the QSO 1225+317 (Pettini *et al.* 1982b) which shows multiple components in two redshift systems at $z_a = 1.62$ and 1.79.

For 0215+015, from a total of nine adjacent pairs of well-determined C IV components in the redshift systems $z_a = 1.345$, 1.549 and 1.649 we find that their average splitting is 113 km s^{-1} which is approximately twice the resolution of the data. This may imply (Bahcall 1975) that there are many more components separated by velocity intervals smaller than our resolution. Bearing this in mind, we have derived ion column densities by fitting theoretical profiles to those absorption lines which have been observed at high resolution and with sufficient signal-to-noise. In this procedure we assume the distribution of the velocities of the ions to be of the form:

$$\psi(v) = \frac{1}{\sqrt{\pi}} \sum_i p_i/b_i \exp [\![-[v - v_0(i)]^2/b_i^2]\!]$$

where i is the number of discrete components contributing to an absorption line, each with central velocity $v_0(i)$, dispersion parameter $b_i = \sqrt{2}\,\sigma_i$ (σ_i being the line-of-sight component of the velocity dispersion) and fraction p_i of the total column density of absorbers, such that

$$\sum_i p_i = 1.$$

Theoretical line profiles are computed from the equations given by Strömgren (1948) for a set of values of the parameters v_0, b and p and compared with the observed absorption features, after convolution with the appropriate instrumental broadening function (measured from narrow comparison arc lines). The process is repeated through several iterations until a satisfactory match is obtained between computed and observed profiles.

In fitting the multiple absorption lines in 0215+015 we have set i equal to the number of components at least partially resolved, and fixed the zero point of the relative velocity scale appropriate to each line by reference to the central wavelength of the strongest component in the line. Each pair of doublet lines has been fitted together yielding a self-consistent model set of parameters, apart from cases where we suspect that one of the lines may be contaminated by unidentified features. Since even apparently single components may in fact be unresolved blends of absorption from multiple absorbing regions, we have fitted each component with the largest b value consistent with the observed profile; this procedure then yields a lower limit to the column density N of the corresponding ion. It can be shown (Nachman & Hobbs 1973; Boksenberg, Carswell & Sargent 1979) that if different absorbing regions, with widely different velocity dispersions, contribute to a component, the derived column density is a reliable estimate of the column density of the region with the largest b. Oscillator strengths are from Morton (1978), except for Si II (Shull, Snow & York 1981) and Fe II (Nussbaumer, Pettini & Storey 1981).

We now describe in turn the four redshift systems and our results from the line profile fitting where applicable.

3.2.1 $z_a = 1.254$ system

This system is identified by a single C IV doublet, shown in Figs 3 and 4, with mean equivalent widths of 1.1 Å (λ 1548.19) and 0.8 Å (λ 1550.76). Unfortunately, these lines occur near the edge of both medium- and high-resolution scans, where the signal-to-noise of the data is low; consequently the line profiles are poorly defined and do not warrant a detailed analysis. The lines appear broad and complex; we tentatively identify two components separated by $\simeq 80$ km s^{-1} and with FWHM $\simeq 160$ km s^{-1}, but these estimates

need to be confirmed by further observations. No other lines are detected in this system, including the intrinsically strong Mg II λλ 2796.35, 2803.53 doublet and multiplets UV1, UV2 and UV3 of Fe II, which at this redshift would occur in a spectral region of good signal-to-noise.

3.2.2 $z_a = 1.345$ system

This is a rich, mixed-ionization system: in our spectra we detect 16 lines (Table 3) ranging from C I, Mg II, Al II and Fe II, which in interstellar gas in our Galaxy are normally attributed to neutral (H I) gas, through to highly-ionized species, including C IV, Al III and Si IV. In this system all the lines which have been observed at high resolution show double

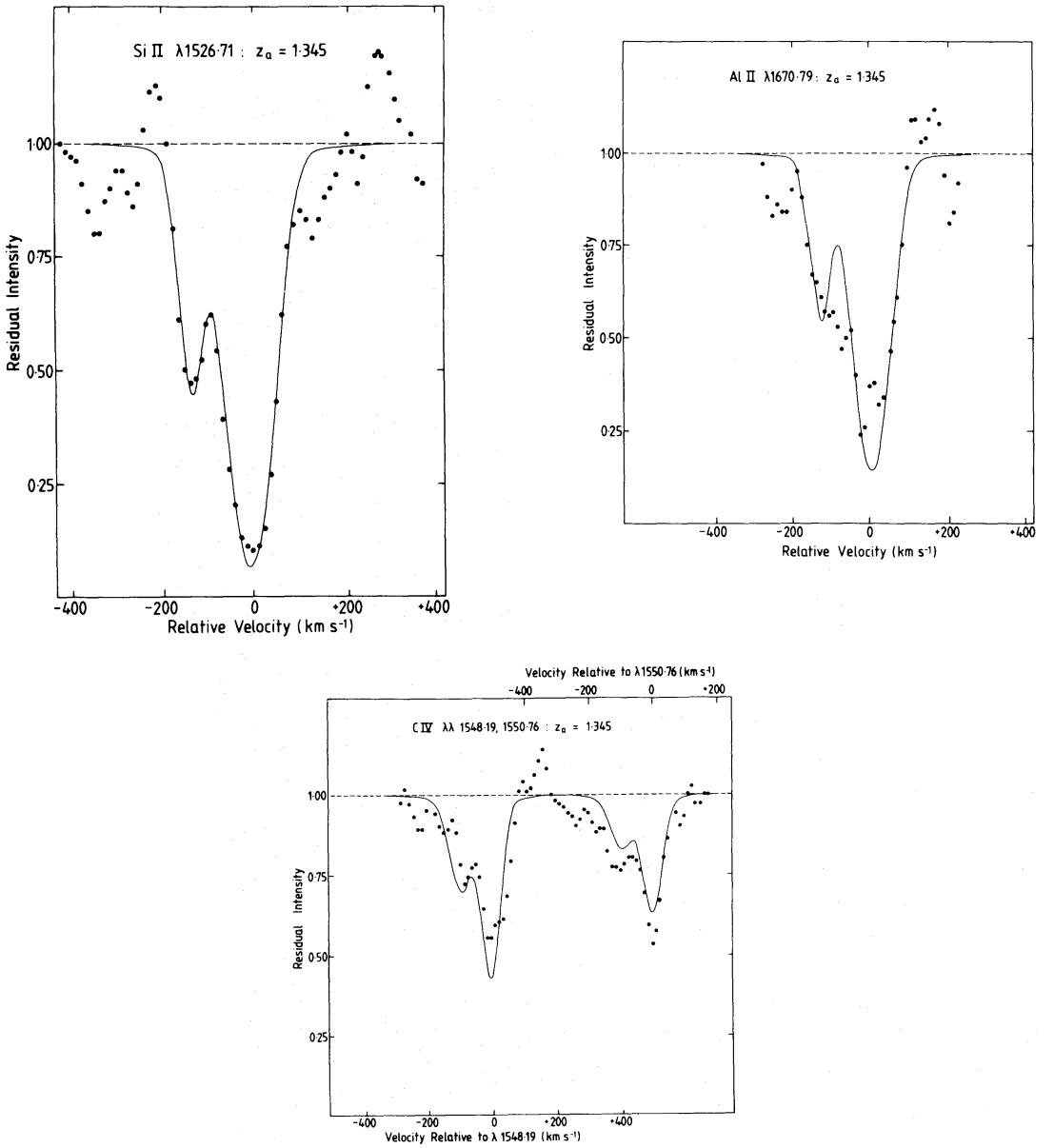

Figure 8. Comparison of the high-resolution data points for lines in the $z_a = 1.345$ system with theoretical line profiles (continuous curve) after convolution with the instrumental profile. In this and the two subsequent figures the data have been normalized to the continuum. The instrumental profile is assumed to be a Gaussian, with FWHM either 0.64 or 0.66 Å depending on the data. The input parameters of the two-component model are given in Table 4.

Table 4. 0215+015: Results of profile fitting for the lines in the $z_a = 1.345$ and $z_a = 1.549$ systems.

λ_{fitted}^{helio} (vac) (Å)	Ident	$\lambda_{rest}^{(vac)}$ (Å)	z	Model parameters		
				Relative velocity (km s^{-1})	b (km s^{-1})	N (10^{13} cm^{-2})
$z_a = 1345$ system						
3578.41	Si II	1526.71	1.34387	−130	20	7.6
3629.54:	C IV	1548.19	1.34438	−96:	35:	3.8:
3635.58:	C IV	1550.76				
—	Al II	1670.79	—	−130	20	0.53
3579.96	Si II	1526.71	1.34489	0	45	34
3630.70:	C IV	1548.19	1.34513	0	25	9.0
3636.74	C IV	1550.76				
—	Al II	1670.79	—	0	45	2.3
$z_a = 1.549$ system						
3944.15	C IV	1548.19	1.54759	−133	30	5.8
3950.70	C IV	1550.76				
3945.90	C IV	1548.19	1.54872	0	55	21
3952.45	C IV	1550.76				
3947.61	C IV	1548.19	1.54983	+130	40	13
3954.18	C IV	1550.76				

Note
The following lines were detected (at high resolution) at the *observed* wavelength indicated below, but were considered too weak to justify model fitting.

$z_a = 1.345$			
3658.69	C I	1560.31	1.34485
3659.99	C I	1560.31	1.34568
$z_a = 1.549$			
3550.23:	Si IV	1393.76	1.5472:
3552.53	Si IV	1393.76	1.54889
3554.38	Si IV	1393.76	1.55022

structure, apart from the Al II λ 1670.79 line which is broad and asymmetric but with the asymmetry in the same sense as the resolved structure of the other lines. The two components have a velocity separation of ~ 100 km s^{-1} determined from an average of the C IV doublet and Si II λ 1526.71 and C I λ 1560.31 lines.

The fits to the complex line profiles are shown in Fig. 8 and the results are listed in Table 4. The Si II λ 1526.71 line is well-reproduced by a two-component model. Application of this model to Al II λ 1670.79 gives a consistent fit bearing in mind that this feature occurs near the edge of the relevant scan where the resolution is somewhat degraded. However, the Si II/Al II model does not fit the profiles of the C IV doublet lines, even allowing for contamination by noise. A reasonably satisfactory fit (considering the weakness of the lines) is obtained with the model parameters given in Table 4 (see Fig. 8). It appears that the low- and high-ionization species are distributed differently within the same redshift system. To confirm this result and to study its implications, we require high-resolution observations of additional species, in particular Mg II, Fe II and Si IV.

Fig. 11 shows that the curve of growth corresponding to the Si II/Al II two-component model fits well the equivalent widths of all the absorption lines detected at $z_a = 1.345$ (apart from the C IV doublet which is not included in the diagram). Thus it appears that the

distribution of Fe II and Mg II, observed only at medium resolution, is similar to that of Si II and Al II. Values of ion column density N derived from the equivalent width data in Table 3 and the curve of growth in Fig. 11 are given in Table 6. The errors in N reflect the scatter of the individual determinations from the mean. Fe II λ 2382.76 was not considered in the derivation of $N(Fe^+)$; this line is strongly saturated and possibly affected by the nearby night sky line at 5577 Å, both factors making the determination of $N(Fe^+)$ from this transition highly uncertain. The Al III lines are weak and yield the same value of $N(Al^{++})$ irrespective of whether the Si II/Al II or the C IV model is assumed. For comparison, ion column densities derived by Gaskell (1982) from lower resolution data and a single component curve of growth with $b = 100\,km\,s^{-1}$ are smaller than the values in Table 6 by factors between ~ 1.5 and ~ 3.

3.2.3 $z_a = 1.549$ system

In the high-resolution spectrum the C IV absorption in this system is triple with component separation $\sim 130\,km\,s^{-1}$ (see Fig. 6). The Si IV λ 1393.76 line is also detected: although weak, the line appears to show a triple structure similar to that of C IV. In particular, the relative strengths of the three components are similar between the two ions, and the velocity separation of the two stronger Si IV components is $\sim +155\,km\,s^{-1}$ which is consistent with the corresponding value found for the C IV doublet. The weaker Si IV λ 1402.77 component will occur very close to the strong Si II λ 1526.71 line in the 1.345 system. There is a possible line at $\lambda_{vac}^{helio} = 3575.9$, corresponding to $z_a = 1.5492$, which is most plausibly the central component of the triple system.

There is a possible absorption feature at 3116 Å in the low-resolution IDS spectrum (see Fig. 2) with $W_\lambda(obs) \sim 5$ Å. If the feature is real then it could be the Ly α 1215.7 Å line in this system. However, the wavelengths in this region are most uncertain because the calibration does not extend below 3180 Å. No other lines from species which are normally found in H I regions are identified in this system.

A three-component model has been fitted to the C IV doublet (see Table 4 and Fig. 9). The agreement is good apart from the lowest redshift component in the λ 1550.76 line; the discrepancy may be due to contamination of the λ 1550.76 component by an unidentified feature. Alternatively, the relative strengths of this feature in λλ 1548.19 and 1550.76 (≃ 1:1) may indicate that it is an unresolved blend of narrow, saturated components. If this were indeed the case, the column density of C IV at this redshift is likely to be substantially higher than the lower limit in Table 4, derived from a single component fit.

3.2.4 $z_a = 1.649$ system

This system contains an exceedingly complex C IV doublet (see Fig. 7) which is not properly resolved at 0.66 Å resolution. At this redshift, lines belonging to the Si IV doublet, C II λ 1334.53 and Ly α are also found.

At 1.5 Å resolution (Fig. 3) the C IV doublet splits into three separate features with central wavelengths of 4100.5, 4016.1 and 4111.4 Å. At higher resolution each of these features splits up into many narrow absorption lines and we make the following identifications. The five, partly resolved, components that constitute the 4100.5 Å feature are attributed to five C IV λ 1548.19 lines. These are labelled A to E in Fig. 7. The two components, $J+K$ and L which consitute the 4111.4 Å feature are identified with two C IV λ 1550.76 components. (The lines J and K are separated by the resolution limit and hence cannot be genuinely resolved; their apparent separation is evidently an artifact of the

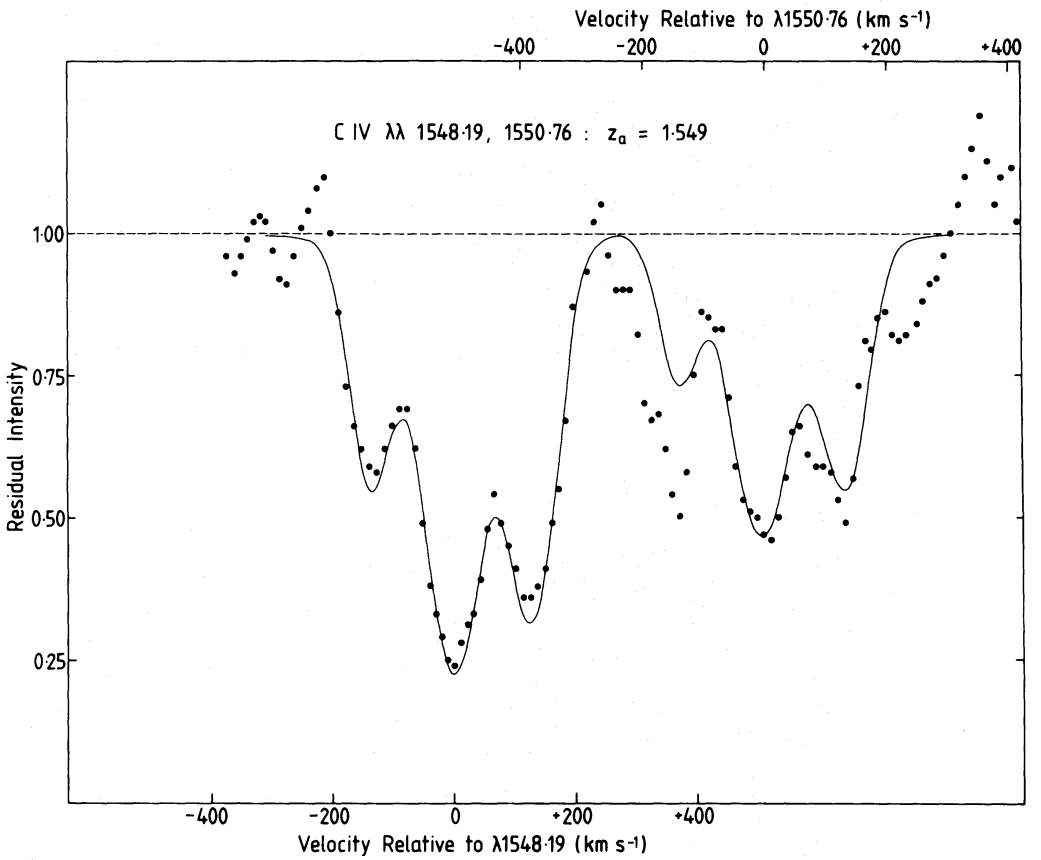

Figure 9. Comparison of the high-resolution $z_a = 1.549$ C IV data with the theoretical model, assuming three components. Input parameters are contained in Table 4.

Table 5. 0215+015: Results of profile fitting for the C IV doublet in the $z_a = 1.649$ system.

λ^{helio}_{fitted} (vac) Å	λ_{rest} (vac) Å	z	Model parameters		
			Relative velocity (km s^{-1})	b (km s^{-1})	N (10^{13} cm^{-2})
4096.92 (*A*)	1548.19	1.64626	−336	15	1.8
—	—				
4097.97 (*B*)	1548.19	1.64694	−259	20	3.7
—	—				
4099.02 (*C*)	1548.19	1.64762	−182	15	3.9
—	—				
4100.12 (*D*)	1548.19	1.64833	−102	23	6.9
—	—				
4101.51 (*E*)	1548.19	1.64923	0	29	10.5
4108.33 (*H*)	1550.76				
—	—	1.65095	+194	25	4.4
4110.99 (*J* + *K*)	1550.76				
—	—	1.65205	+319	20	2.2
4112.70 (*L*)	1550.76				

Note
The letters following the λ^{helio}_{fitted} values in column one correspond to those shown in Figs 7 and 10.

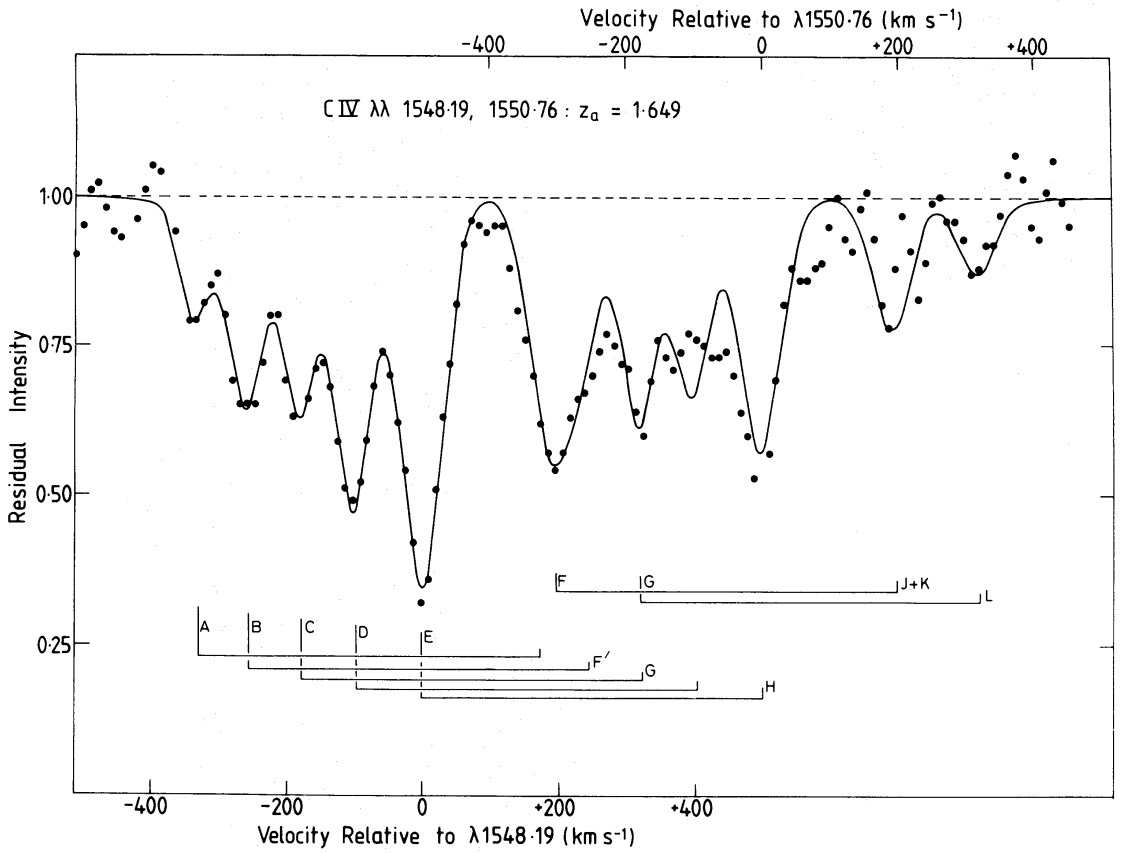

Figure 10. Comparison of the high-resolution $z_a = 1.649$ C IV data with the theoretical model, assuming seven components with relative velocities as shown. Input parameters are contained in Table 5.

noise.) Then, the 4106.1 Å feature must consist of the five C IV λ 1550.76 components from the first mentioned complex as well as the two C IV λ 1548.19 components from the 4111.4 Å feature. On this basis, we identify seven separate C IV systems covering a redshift range of $\Delta z \sim 0.005$ which corresponds to a velocity range of $\sim 650\,\mathrm{km\,s^{-1}}$.

A seven-component model, consistent with the above interpretation, has been fitted to the C IV doublet (see Table 5 and Fig. 10). The agreement is good apart from the region between components *G* and *H* (see Fig. 7) and *J* + *K* which has already been discussed. We point out that all the components are remarkably narrow, with $15 \leqslant b < 30\,\mathrm{km\,s^{-1}}$ By comparison, the C IV components in the 1.549 system have $30 \leqslant b \leqslant 55\,\mathrm{km\,s^{-1}}$.

Structure also occurs in the Si IV doublet and C II λ 1334.53 line. Both of the Si IV lines are double with the stronger component having a FWHM $\sim 180\,\mathrm{km\,s^{-1}}$, whilst the C II line is probably triple with FWHM $\sim 400\,\mathrm{km\,s^{-1}}$. Better quality spectra are required to allow identification of these species with any of the seven C IV subsystems.

A very strong Ly α line at $z_a \simeq 1.647$ and $W_\lambda = 15$ Å also belongs to this system (see Fig. 2). The present IDS observations of this line are at too low a resolution to show any component structure on the same scale as the C IV complex.

4 Discussion

We have observed four definite absorption systems in 0215+015, all of which show complex structure at high resolution, the degree of complexity generally increasing with redshift.

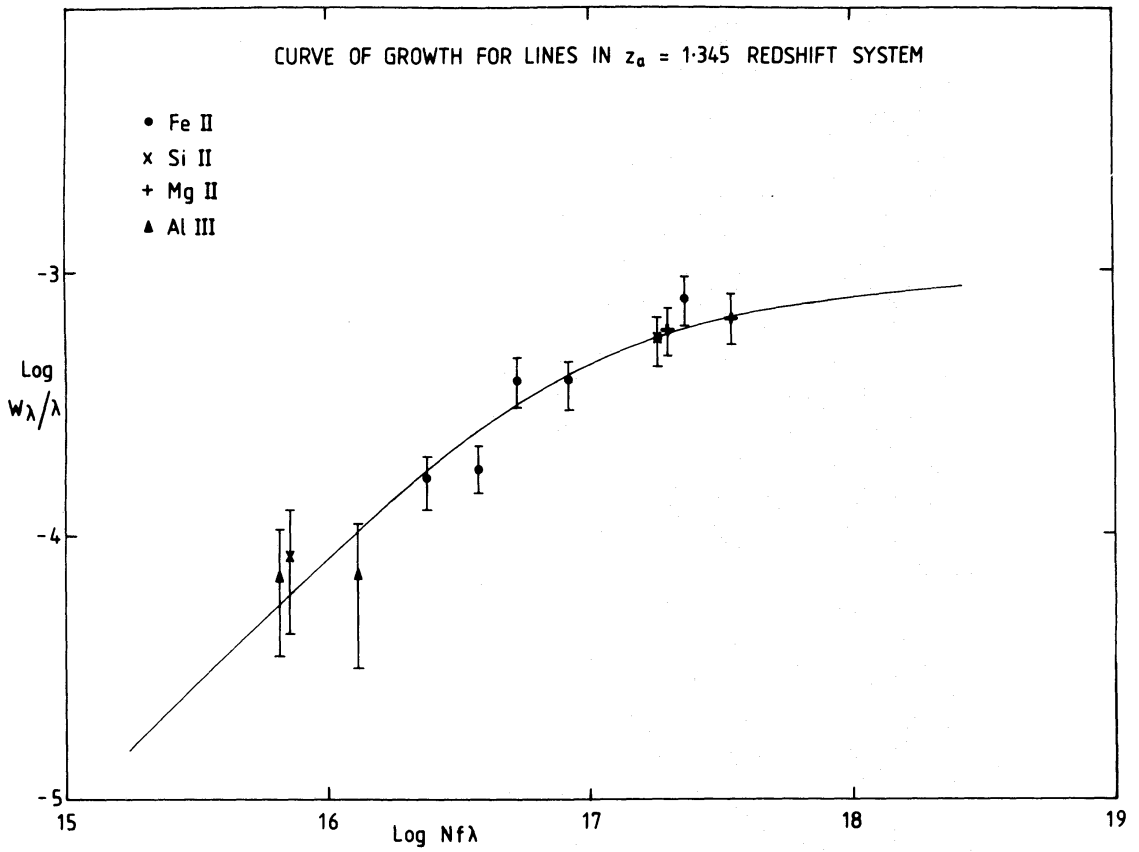

Figure 11. Curve of growth appropriate to the two-component model of ion velocities derived from fitting the profiles of the Si II and Al II lines in the $z_a = 1.345$ system (see Fig. 8). Model parameters are given in Table 4. Equivalent widths of absorption lines belonging to this redshift system generally fit well the curve of growth for this model, apart from the C IV doublet (not shown) which is apparently distributed differently from the other ions. Equivalent widths of lines observed in more than one spectrum (see Table 3) are weighted means of the individual measurements.

There is one mixed-ionized system at $z_a = 1.345$ and three systems dominated by C IV absorption at $z_a = 1.254$, 1.549 and 1.649. The redshift of the object is unknown since no emission features have been detected, but it is clearly a highly luminous object. At the time of the 1980 September observation, its luminosity at 2000 Å in the emission frame of the object was at least 7×10^{29} W Hz^{-1} assuming that $z_{em} \geqslant 1.649$ and adopting $H_0 = 100$ km s^{-1} Mpc^{-1} and $q_0 = 0.5$.

The C IV profiles are especially noteworthy in the high-ionization systems with the $z_a = 1.549$ system splitting into at least three components and the $z_a = 1.649$ system into at least seven components. Fine structure splitting on a velocity scale of 90–180 km s^{-1} are in fact a common feature of C IV doublets in QSO spectra when observed at sufficiently high resolution, as shown clearly in fig. 5 of Sargent *et al.* (1980). Nevertheless, the complexity of the C IV doublet in the $z_a = 1.649$ system is remarkable, these lines showing an unusually large number of narrow, closely spaced components.

An important question concerns the origin of the narrow absorption lines commonly seen in the spectra of QSOs and BL Lac objects. It is argued (see, for example, Bahcall & Spitzer 1969; Sargent *et al.* 1980) that these features arise in cosmologically distributed intervening material either associated with galaxies (metal line systems) or as intergalactic clouds (Ly α systems). Alternatively, the narrow lines may originate in gas that has condensed from material ejected from the central source (e.g. Rees 1970; Dyson *et al.* 1980). The intervening

hypothesis requires that galaxies extend significantly beyond their optical dimensions. That this can indeed be the case has been shown conclusively by the detection of interstellar galaxian Ca II in the QSO-galaxy pair 3C 232–NGC 3067 (Boksenberg & Sargent 1978) and in the spectra of the QSOs 2020 – 370 (Boksenberg *et al.* 1980) and 0446 – 208 (Blades, Hunstead & Murdoch 1981). Quantitatively, it is possible to use the statistics of detection of narrow absorption lines in QSO spectra to infer the required size of galactic haloes (Sargent *et al.* 1979), but the interpretation of the available data is controversial (Burbidge *et al.* 1977). The recent study of a homogeneous, unbiased sample of 33 QSOs by Young, Sargent & Boksenberg (1982) showed that spherical haloes of radii $R_* = 44\ (100/H_0)$ kpc are required to account for the observed incidence of C IV doublets. The corresponding dimensions implied by the frequency of Mg II doublet detections are $R_* = 22\ (100/H_0)$ kpc. If the intervening material is in the form of randomly oriented discs, the required sizes (radii of the discs) are increased by a factor of $\sqrt{2}$.

Currently a considerable effort is being made to determine the gaseous extent of the halo of our Galaxy. A few high-resolution ultraviolet observations of high-latitude gas in our Galaxy have now been made with the *IUE* satellite, including the directions of the Magellanic Clouds (Savage & de Boer 1981), the supernova 1980k in NGC 6946 (Pettini *et al.* 1982a) and the Seyfert nuclei Mkn 509 and F9 (York *et al.* 1982; Pettini *et al.* 1982c). Using the same model of a halo corotating with the galactic disc, these studies, which probe different sight-lines, obtain the same result, namely that interstellar gas extends up to ~ 10 kpc from the galactic plane over a large area of the disc (in one case up to 50 kpc from the Sun). These results are based on indirect arguments and are limited to a few directions. They do not necessarily provide support for the existence of galactic haloes of sufficient extent to account for the frequency of occurrence of QSO absorption systems.

The intervening hypothesis can be investigated further by comparing the characteristics of absorption produced by galactic halo gas with those of redshift systems in QSOs and BL Lacs. The most useful comparisons, at present, can be made between the *IUE* high-resolution studies of early-type stars in the Magellanic Clouds and the spectra of a few QSOs and BL Lac objects which have been observed at sufficiently high resolution. A recent study along these lines by Savage & Jeske (1981) has revealed remarkable similarities between absorption systems in the galactic halo and in high-redshift QSOs. We are now able to extend the comparison by including the present data on 0215+015.

We will consider first the $z_a = 1.345$ system. In Table 6 the column densities derived for this system are compared with those derived by Savage & de Boer (1981) for the galactic halo in the direction of HD 36402 in the LMC and also with those given by Young *et al.* (1979) for the $z_a = 2.7685$ system in the QSO 2126 – 158. Differences of ~ 20 per cent will occur amongst the column densities given in Table 6 due to the use, in some cases, of different oscillator strengths. In the present context these differences are insignificant.

It is important to bear in mind that large errors can arise in column densities determined via a curve of growth; in particular, the method can underestimate the true column density when components with small velocity widths but significant columns go undetected. Notwithstanding this caveat, there is remarkable agreement between the column densities found here for the $z_a = 1.345$ system in 0215+015 and those found by Savage & Jeske (1981) for the galactic halo. This makes an extremely strong case for considering this system as due to an intervening galaxy (a similar conclusion was reached by Gaskell 1982, but our improved modelling based on higher-resolution data has given an even better fit). Savage & Jeske considered that their results for the galactic halo compared remarkably well with those of Young *et al.* (1979) for the $z_a = 2.7685$ system in 2126 – 158 and also noted that this gave the closest agreement from among several QSO absorption systems studied at high

Table 6. Comparison of ion column densities between the $z_a = 1.345$ system in 0215+015, the halo of the Galaxy and a high redshift QSO absorption system.

Species	$\lambda_{rest}^{(vac)}$ Å	f	Column densities		
			0215+015 $z_a = 1.345$ 10^{13} cm^{-2}	Galactic halo toward HD 36402 10^{13} cm^{-2}	2126−158 $z_a = 2.7685$ 10^{13} cm^{-2}
C IV	1550.76	0.097	12 ± 2	10	50
	1548.19	0.194			
Mg II	2803.53	0.295	24 ± 3	30	—
	2796.35	0.592			
Al II	1670.79	1.88	3.3 ± 0.8	1.5	1.7
Al III	1862.79	0.268	1.3 ± 0.5	—	—
	1854.72	0.539			
Si II	1808.01	0.0055	60 ± 15	35	18
	1526.71	0.20			
Fe II	2600.18	0.294	24 ± 6★	25	20
	2586.65	0.0846			
	2382.76	0.396			
	2374.46	0.0419			
	2344.21	0.15			
	1608.46	0.0963			

★ Mean of five lines excluding the λ 2382.76 line (see text).

resolution. The agreement with the $z_a = 1.345$ system in 0215+015 is, however, even better. There is an order of magnitude difference in the ratio of the column densities of C IV to those of Si II between the results for either the galactic halo or 0215+015 and those for 2126−158.

As Savage & Jeske point out, our sight-line to the LMC commences 8.5 kpc from the centre of our Galaxy. It may well be that the sight-line to 0215+015 happens to pass fairly close (~ 10 kpc) to the centre of the intervening galaxy responsible for the $z_a = 1.345$ system. If galaxies do indeed have haloes $\gtrsim 30$ kpc, a more typical sight-line might well pass through the outer halo leading to a higher proportion of C IV and less Si II. In this regard it is interesting to note that our results suggest (see Table 3) that the low- (Si II) and high- (C IV) ionization species may be distributed differently within the overall system. A similar result was found for the low and high ions in the haloes of the Galaxy and of the Magellanic Clouds (de Boer & Savage 1980; Savage & de Boer 1981).

The three high-ionization systems are quite different in character from the $z_a = 1.345$ system. They are all dominated by C IV, whilst Si II (λ 1526.71) is not detected, although the strongest line (λ 1260.42) is outside the wavelength range covered by our spectra. This suggests a combination of high temperature and/or lower metallicity. The $z_a = 1.649$ system differs from the $z_a = 1.549$ system in having a lower average dispersion parameter b. For $z_a = 1.649$, b ranges from 15 to 29 km s^{-1} with average value 21 ± 2 km s^{-1} whilst for $z_a = 1.549$ it ranges from 30 to 55 km s^{-1}. A word of caution is necessary here in that it is by no means certain that either system has been fully resolved.

In the $z_a = 1.649$ system the b values of ~ 20 km s^{-1} and the observed component separations agree remarkably well with the predictions of the ejection model of Dyson *et al.* (1980). Briefly, this work shows that a wind from a central source (QSO nucleus) will sweep

up ambient material which at some characteristic time cools radiatively and condenses into thin shells. These are likely to break up into sub-shells with velocity differences in the range 50–120 km s^{-1} and linewidths of ~ 20 km s^{-1}.

Young *et al.* (1982) present evidence for the existence of shells of ejected material in QSOs with broad absorption troughs, of which PHL 5200 is the archetype. Such ejected material gives rise to narrow absorption lines which differ from the more commonly seen sharp lines in that, (a) they cluster near the emission redshift; (b) they are broader than the sharp lines, with typical widths of 250–500 km s^{-1} (FWHM); (c) the ionization level is high and N V is commonly seen. Although we cannot at present establish if points (a) and (c) apply to the $z_a = 1.649$ system in 0215+015, we note that the overall width of the C IV doublet lines is similar to that of the ejected QSO lines. There are indeed striking similarities between the C IV feature in our medium resolution spectrum (Fig. 3) and the ejected lines in the spectrum of Q1309−056 at 2.5 Å resolution (fig. 1 of Young *et al.* 1982). Clearly, it is of great interest to (i) extend our observations of the $z_a = 1.649$ system in 0215+015 to include the region of the N V lines, and (ii) to observe ejected lines in trough QSOs at sufficiently high dispersion to resolve their intrinsic structure.

We now consider the possibility that the $z_a = 1.649$ system arises in intervening material. The rms dispersion of the seven components is 240 km s^{-1}. Since this is near the lower limit of the range of dispersions given by Yahil & Vidal (1977) for low-redshift clusters (viz. ~ 100 to 1400 km s^{-1}), a possible interpretation is that each component represents absorption in a separate galaxy in a cluster. This, however, seems unlikely since: (1) the b values are rather small if each component results from the sight-line passing through the halo of a galaxy corotating with its disc and (2) the velocity separations are fairly uniform although this may be forced by the instrumental resolution as mentioned earlier.

If, on the other hand, the complex absorption in the $z_a = 1.649$ system of 0215+015 is due to a single galaxy, then the separate components would arise in individual clouds of gas within the halo. Unfortunately, there is little information on the structure of outer haloes of galaxies. Available data on the profile of C IV absorption in our Galaxy and in the Magellanic Clouds (Gondhalekar *et al.* 1980; Savage & de Boer 1981) do not indicate the complex structure needed to explain the $z_a = 1.649$ system in 0215+015. On balance we tend to favour the ejection interpretation for this system because of the close agreement with the model of Dyson *et al.* and the apparent similarities with the shell lines in QSOs with troughs.

The $z_a = 1.549$ system has, on an ejection model, a velocity of at least 11 500 km s^{-1}, a value consistent with the observations of Young *et al.* (1982). Its b values do not fit the Dyson *et al.* model as well as those of the 1.649 system. Either possibility (intervening or intrinsic) seems equally plausible here. As already noted, there may well be unrevealed additional structure in this system, and there is a definite need for even higher-resolution observations.

The $z_a = 1.254$ system presents more of a problem for the ejection model. This system is also a C IV-dominated system. The C IV in this system has not been studied in the same detail as the other two as it is weaker and furthermore occurs in a region of lower signal-to-noise. Nevertheless, it clearly has double structure. Any claim that the complex C IV-dominated systems are all ejected must face up to separate systems with widely-separated ejection velocities but very narrow velocity components within each system. The high 'ejection velocity' of the $z_a = 1.254$ system argues against the ejection hypothesis and thereby in favour of absorption by an intervening galaxy, and hence for the existence generally of complex C IV systems in the outer haloes of intervening galaxies. Nevertheless, there is a plausible case for believing that at least the $z_a = 1.649$ system is due to material ejected from the central object, because of its extreme complexity. It is interesting to note that in each

of the high-redshift BL Lac objects, 0215+015 and 1309−216 (Blades *et al.* 1980) the highest-redshift system has very strong complex C IV absorption.

Additional high-resolution data are needed for many of the lines already detected in 0215+015. In particular, high signal-to-noise observations of Ly α, N V and Si IV in the two highest-redshift systems are needed to interpret fully the complex C IV absorptions and to obtain information on the temperature of the absorbing medium. Observations of the near UV with *IUE* should allow a search for O VI lines at $z_a = 1.649$ and $z_a = 1.549$. Finally, high-resolution observations of the remaining lines in the $z_a = 1.345$ system are needed for a detailed abundance analysis. As the object appears to be currently in a bright phase it is important to obtain these data as soon as possible.

Acknowledgments

We are grateful to C. M. Gaskell for providing us with details of his Lick Observatory study of 0215+015 ahead of publication. We thank J. J. Condon for communicating his unpublished VLA observations and D. Carter for obtaining the red-region spectrum. R. W. Hunstead and H. S. Murdoch acknowledge support from the Australian Research Grants Committee. The AAT time was largely provided by the Australian Time Assignment Committee, and we are grateful for their continuing support.

References

Bahcall, J. N., 1975. *Astrophys. J.*, **200**, L1.
Bahcall, J. N & Spitzer, L. Jr., 1969. *Astrophys. J.*, **156**, L63.
Bentley, M., Haves, P., Spencer, R. E. & Stannard, D., 1976. *Mon. Not. R. astr. Soc.*, **176**, 275.
Blades, J. C., 1980. *Users Guide to the RGO Spectrograph*, AAO publication.
Blades, J. C., Hunstead, R. W. & Murdoch, H. S., 1981. *Mon. Not. R. astr. Soc.*, **194**, 669.
Blades, J. C., Murdoch, H. S. & Hunstead, R. W., 1980. *Mon. Not. R. astr. Soc.*, **191**, 61.
Boksenberg, A., 1978. *Proc. ESO Conference, Telescopes of the Future, Geneva, 1977 December 12–15*, p. 497.
Boksenberg, A., Carswell, R. F. & Sargent, W. L. W., 1979. *Astrophys. J.*, **227**, 370.
Boksenberg, A., Danziger, I. J., Fosbury, R. A. E. & Goss, W. M., 1980. *Astrophys. J.*, **242**, L145.
Boksenberg, A. & Sargent, W. L. W., 1978. *Astrophys. J.*, **220**, 42.
Bolton, J. G. & Wall, J. V., 1969. *Astrophys. Lett.*, **3**, 177.
Bolton, J. G. & Wall, J. V., 1970. *Aust. J. Phys.*, **23**, 789.
Burbidge, G., O'Dell, S. L., Roberts, D. H. & Smith, H. E., 1977. *Astrophys. J.*, **218**, 33.
Condon, J. J. & Jauncey, D. L., 1974. *Astr. J.*, **79**, 1220.
Cotton, W. D., Wittels, J. J., Shapiro, I. I., Marcaide, J., Owen, F. N., Spangler, S. R., Rius, A., Angulo, C., Clark, T. A. & Knight, C. A., 1980. *Astrophys. J.*, **238**, L123.
de Boer, K. S. & Savage, B., 1980. *Astrophys. J.*, **238**, 86.
Dyson, J. E., Falle, S. A. E. G. & Perry, J. J., 1980. *Mon. Not. R. astr. Soc.*, **191**, 785.
Gaskell, C. M., 1978. *Bull. Am. astr. Soc.*, **10**, 663.
Gaskell, C. M., 1982. *Astrophys. J.*, **252**, 447.
Gondhalekar, P. M., Willis, A. J., Morgan, D. H. & Nandy, K., 1980. *Mon. Not. R. astr. Soc.*, **193**, 875.
Hunstead, R. W. & Murdoch, H. S., 1980. *Mon. Not. R. astr. Soc.*, **192**, 31P.
Large, M. I., Mills, B. Y., Little, A. G., Crawford, D. F. & Sutton, J. M., 1981. *Mon. Not. R. astr. Soc.*, **194**, 693.
Morton, D. C., 1978. *Astrophys. J.*, **222**, 863.
Nachman, P. & Hobbs, L. M., 1973. *Astrophys. J.*, **182**, 481.
Nussbaumer, H., Pettini, M. & Storey, P. J., 1981. *Astr. Astrophys.*, **102**, 351.
Oke, J. B., 1974. *Astrophys. J. Suppl.*, **27**, 21.
Pettini, M., Benvenuti, P., Blades, J. C., Boggess, A., Boksenberg, A., Grewing, M., Holm, A., King, D. L., Panagia, N., Penston, M. V., Savage, B. D., Wamsteker, W. & Wu, C.-C., 1982a. *Mon. Not. R. astr. Soc.*, **199**, 409.

Pettini, M., Boksenberg, A., Sargent, W. L. W. & Carswell, R. F., 1982b. In preparation.
Pettini, M., Penston, M. V., Boksenberg, A., Snijders, M. A. J., Sargent, W. L. W. & Gull, T. 1982c. In preparation.
Rees, M. J., 1970. *Astrophys. J.*, **160**, L29.
Robinson, L. & Wampler, E. J., 1972. *Publs astr. Soc. Pacif.*, **84**, 161.
Sargent, W. L. W., Young, P. J., Boksenberg, A., Carswell, R. F. & Whelan, J. A. J., 1979. *Astrophys. J.*, **230**, 49.
Sargent, W. L. W., Young, P. J., Boksenberg, A. & Tytler, D., 1980. *Astrophys. J. Suppl.*, **42**, 41.
Savage, B. D. & de Boer, K. S., 1981. *Astrophys. J.*, **243**, 460.
Savage, B. D. & Jeske, N. A., 1981. *Astrophys. J.*, **244**, 768.
Shull, J. M., Snow, T. P. & York, D. G., 1981. *Astrophys. J.*, **246**, 549.
Straede, J., 1980. *An Approach to the Reduction of Digital Spectral Data,* AAO preprint No. 135.
Strömgren, B., 1948. *Astrophys. J.*, **108**, 242.
Wall, J. V., 1972. *Aust. J. Phys., Astrophys. Suppl.*, **24**, 1.
Wills, D., 1979. *Astrophys. J. Suppl.*, **39**, 291.
Wills, D. & Lynds, R., 1978. *Astrophys. J. Suppl.*, **36**, 317.
Wyllie, D. V., 1969. *Mon. Not. R. astr. Soc.*, **142**, 229.
Yahil, A. & Vidal, N. V., 1977. *Astrophys. J.*, **214**, 347.
York, D. G., Blades, J. C., Cowie, L. L., Morton, D. C., Songaila, A. & Wu, C.-C., 1982. *Astrophys. J.*, **255**, 467.
Young, P. J., Sargent, W. L. W. & Boksenberg, A., 1982. *Astrophys. J. Suppl.*, in press.
Young, P. J., Sargent, W. L. W., Boksenberg, A., Carswell, R. F. & Whelan, J. A. J., 1979. *Astrophys. J.*, **229**, 891.